energies

MDPI

Article

Simulation of Combined Aging Effects for Battery Operated Trains: A Benchmark Case Study on the Line Between Reggio Calabria and Catanzaro

Luca Pugi *, Tommaso Elios Povolato and Nico Tiezzi

Department of Industrial Engineering, University of Florence, 50121 Firenze, France; tommaso.povolato@edu.unifi.it (T.E.P.); nico.tiezzi1@edu.unifi.it (N.T.)
* Correspondence: luca.pugi@unifi.it

Abstract: The expected life and reliability of components is a critical aspect for railway applications where the expected life and maintenance intervals of rolling stock are quite demanding issues both in terms of equivalent mileage and duration. For these reasons, when the mileage of the mission is within 100 km, adopted accumulators are based on lithium titanate chemistry, which, despite a relatively low density, ensures a very long operational life both in terms of cycle and time aging. In this work, the authors introduce a benchmark test case, an Italian line between Reggio Calabria and Catanzaro, in which the required autonomy, more than 170 km, involves the usage of high-energy batteries such as LiNMC or $LiFePO_4$ derived from corresponding automotive applications. In this work, the authors propose a simulation model based on IEC 62864-1:2016 to investigate how the combined effect of cycle and time aging should influence in different ways the design of the system and how relatively small interventions such as the partial electrification of a small intermediate section of the line should improve the overall stability and reliability of the performed engineering analysis.

Keywords: battery-operated rolling stock; simulation of multimodal trains; IEC 62864-1:2016; design sensitivity to cycle and time aging; partially electrified lines; mechatronics; direct and inverse dynamic modeling of longitudinal train dynamics

Academic Editor: JongHoon Kim

Received: 4 February 2025
Revised: 19 February 2025
Accepted: 19 February 2025
Published: 26 February 2025

Citation: Pugi, L.; Povolato, T.E.; Tiezzi, N. Simulation of Combined Aging Effects for Battery Operated Trains: A Benchmark Case Study on the Line Between Reggio Calabria and Catanzaro. *Energies* **2025**, *18*, 1143. https://doi.org/10.3390/en18051143

1. Introduction

The electrification of railway lines offers the possibility of removing most of the local direct CO_2 emissions of rolling stock, however, involved maintenance and construction costs are often justified only by relatively high traffic flows [1]. Data concerning the diffusion of electrified lines and, more generally, adopted electrification standards are currently accessible from various national and international data repositories. For the purpose of this work, most of these data have been taken from a free public repository, "OpenRailwayMap" [2], which is a substantially detailed online map of the world's railway infrastructure, built with OpenStreet Map data, some of these data can be easily further, accessed and processed using large language models [3]. As shown in Figure 1, the diffusion of electrified lines is still affected by complex geo-political issues related not only to the cost of energy, climate and internal demography of countries but also by historical and political choices. For example, extensively electrified networks should be found in highly industrialized countries such as the ones of the BENELUX area, but also in emerging powers such as India or even in countries that suffer from persistent industrial and political isolation such as North Korea. At the same time, the persistence of not electrified lines in many highly

developed countries is often a matter of opportunity in terms, as an example of economic sustainability. Climate and sustainable development goals should boost the diffusion of electrified lines, involving large investments that should be only partially justified in terms of terms of economic return. In this sense, the adoption of battery-operated [4,5] or hybrid trains [6,7] represents an interesting perspective to reduce direct emissions with reduced investments and infrastructural impacts on the territory. In addition, recent studies [8] in which the overall sustainability of different solutions is compared clearly indicate that in many different operational scenarios, both battery-operated and hybrid trains should be more sustainable when considering the environmental impact of the infrastructure. The impact on sensitive natural or historical sites should also be considered unacceptable. For all these reasons, there is a growing interest in the development of studies in which the optimization of battery-operated and fuel-cell systems is performed for a specific train over a specific mission profile, as in the recent work of Fragiacomo et al. [9]. In addition, this analysis can also be completed considering some preliminary evaluations of the aging of the components, as performed as an example by Spedicato [10]. The same problem, the compensation of aging effects of critical components such as fuel cells, is also the object of recent works in which this issue is managed with extensive use of artificial intelligence as proposed by Deng et al. [11] or by other authors studying batteries [12,13].

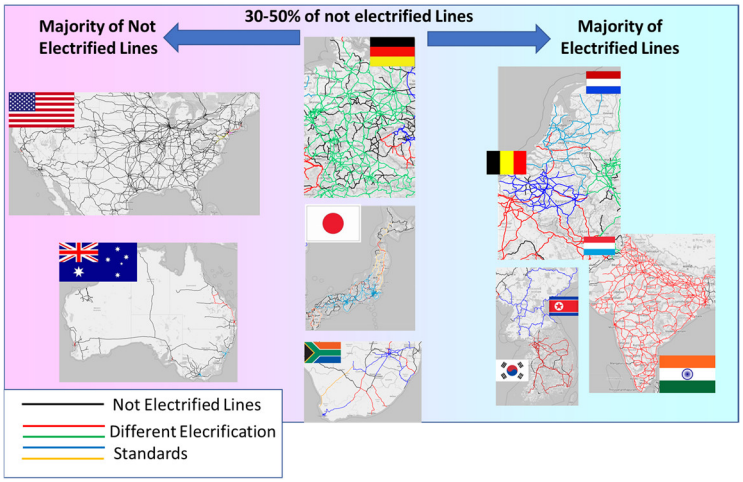

Figure 1. Diffusion of Electrified and Not Electrified Lines in different countries, some examples from free data available online [2].

Other recent works, such as the one of Vignati [14], concern the integration of hybrid and battery-operated powertrains that concern unmanned driverless systems used for diagnostic purposes and also under electrified lines.

In this work, the authors focus their attention on the simulation of battery operating rolling stock with particular attention to a new emerging category of BEMUs (Battery Electric Multiple Units) designed to reach maximum autonomies between 200 and 300 km to cover the exercise over partially or not electrified lines in which the required autonomies without external recharge are over 150 km. This focus on local passenger traffic is justified by the specific features of the railway market in Italy and, more generally, in Western Europe that privilege the application of battery-operated rolling stock to local passenger transportation, but similar technologies can also be applied to freight trains [15].

To reach this objective, the size of installed batteries should significantly grow with respect to conventional autonomies of 50–100 km: in this kind of application, reliability and durability specifications that are typical of the railway sectors are obtained by installing LTO (Lithium Titanate) battery packs which assure a cycle life over 10,000 cycles and probably the highest stability in terms of time aging [16]. Chemistries currently used for

automotive applications, such as LiNMC and $LiFePO_4$, offer much higher energy densities, being much cheaper with respect to their LTO counterparts [17,18]. However, their expected life in terms of equivalent charge and discharge cycles is often limited (2000–4000 cycles), and sensitivity to calendar aging is typically higher [19]. In addition, thermal stability and, more generally, reliability vs. off-design conditions are a bit more critical for LiNMC batteries with respect to LTO ones. So, in this work, the authors focused their attention on the preliminary simulation of a benchmark BEMU on an Italian Line from Reggio Calabria to Catanzaro Lido, for which an extended autonomy of at least 150 km is required. This line is a well-known benchmark offering the possibility of a comparison with other studies related, for example, to the application of hydrogen-powered rolling stock [9]. With regard to the proposed benchmark train, the authors considered a BEMU inspired by the existing Blues–Masaccio Platform, for which a large amount of free information are freely available online [20–22]. In addition, in this case proposed rolling stock offers the possibility of further comparisons with previous studies [23] regarding the application of fuel cell technology, which is probably one of the most important concurrent technologies that concern both autonomy and sustainability.

Different kinds of storage systems can be installed on railway rolling stock. For the purpose of this work, attention is focused on electrochemical batteries and lithium chemistries that should be considered the best candidates for this kind of application, including LTO (Lithium Titanate) and LiNMC (Lithium Nickel, Manganese, Cobalt).

The two chemistries are almost equivalent in terms of total stored energy during the expected battery life. The specific energy of a cell E_{spec} represents the quantity of energy that can be stored per unit of mass. Neglecting calendar aging life can be expressed in terms of an equivalent number of charge and discharge cycles. The total quantity of energy that can be stored per mass unit during the entire life of the cell is represented by $E_{spec\_Ncycles}$ (1).

$$E_{spec\_Ncycles} = E_{spec} N_{cycles} \quad (1)$$

The corresponding comparison of the two chemistries in terms of $E_{spec\_Ncycles}$ is shown in Table 1, demonstrating their substantial equivalence.

Table 1. Expected Total Stored Energy during the life of batteries with different chemistries (mean data referred to assembled batteries).

Chemistry	Specific Energy	Number of Cycles	Total Stored Energy
LiNMC	200 [Wh/kg]	2500–4000	500,000–800,000 [Wh/kg]
LTO	50 [Wh/kg]	10,000–16,000	500,000–800,000 [Wh/kg]

So, the idea that guides this research is to use LiNMC batteries to obtain storage which has the same weight as conventional LTO storage and the same life in terms of mileage/service duration. Beyond this equivalence, the autonomy assured by a LiNMC battery with a single battery recharge is much higher since the capacity of the storage is much higher.

So, it can be concluded that the adoption of LiNMC storage should offer the possibility of performing longer missions with respect to LTO ones, without penalizing the life of the battery too much. The validity of this approach must be verified with simulation tools able also to verify the effect of calendar aging which is substantially negligible for LTO batteries but not for LiNMC ones.

The analysis is performed with the following steps:

- The train model and adopted simulation platform are introduced.

- Then, the battery is sized with respect to the available load capabilities of the benchmark rolling stock.
- Then, a simulation campaign is performed to evaluate the combined effect of cycle and calendar aging of the kind and sizes of the battery pack.
- Finally Obtained results are critically evaluated, concluding the work.

2. Adopted Train Model

The behaviour of the simulated rolling stock is performed by adopting a Matlab–Simulink (release 1.0) model that reproduces the general powertrain scheme that is currently proposed by regulations in force, such as the Standard IEC 62864-1:2016 [24], as shown in Figure 2; the model is divided into six sub-models that can be combined in different ways to simulate different multimodal powertrains:

- Traction Equipment: calculation of consumed or regenerated power P_{TE} according to mission profile.
- Brake Resistor: calculation of the power P_{BR} that should be dissipated during a braking manoeuvre.
- Auxiliaries: calculation of consumptions of auxiliaries P_{AUX} such as HVAC or pneumatic brake compressors.
- Primary Power Source: in the multi-modal hybrid system, the primary power source is the main source of power (P_{PPS}) of the system; it should be a prime mover such as a fuel cell or a diesel motor or the external connection (as an example the pantograph) with an external source of electrical power. For the purpose of this work, the primary source is the pantograph for service under the electrified line or other devices for fast recharge in standstill conditions.
- Energy Storage ESS: in every multimodal system, there is the need for storage working as a power/energy buffer. From a physical point of view, this sub-model corresponds to the model of an electrochemical (battery) or electro-static (capacitor) storage able to exchange the power P_{ESS}. For the purpose of this work, investigated batteries are the storage.
- Power Management Logic: this sixth block/model is not represented by the scheme usually adopted by regulation by IEC 62864-1:2016, but it is as fundamental as the other ones since it represents the logic that regulates the power flow exchanges between the over-described elements.

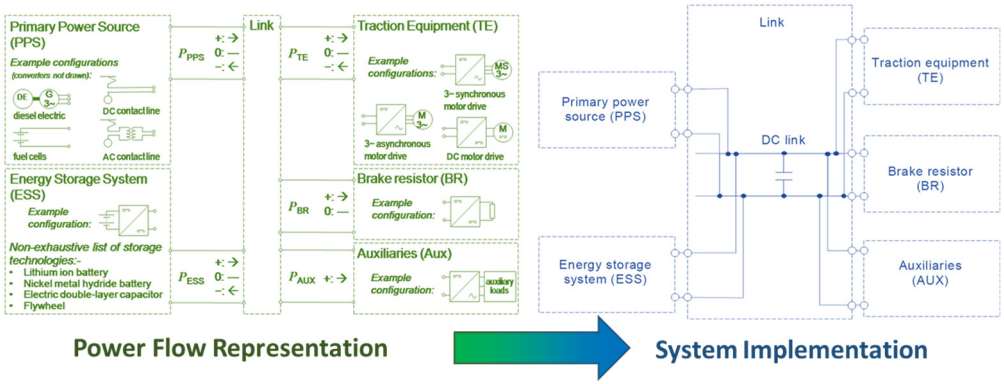

Figure 2. Power Flow (**Top**) Representation and corresponding general system implementation (**bottom**).

2.1. Traction Equipment Block

Calculating the traction loads associated with mission profiles is fundamental to reproducing a realistic mission profile starting from an assigned timetable, respecting constraints imposed by the infrastructure by traction and braking performances.

Vehicle dynamics can be solved using both a direct dynamic approach and an inverse dynamic one. Referring to previous studies cited in this paper [4,7,9], most of the work found in the literature adopts a direct approach in which the Davis model (2) is directly solved, especially when the object of the investigation is to evaluate how engineering constraints such as battery state or interaction with other external constraints (as example power limitations on catenary) should affect the performed mission [25,26]:

$$mk_i\ddot{x} = T(\dot{x}, k_m) - mgi(x) - mgi_c(x) - mg(a\dot{x}^2 + b\dot{x} + c) - d(\dot{x} + \dot{x}_w)^2 \quad (2)$$

Otherwise, if the attention is focused on the precise reproduction of a timetable, the inverse dynamic approach is preferable. Currently, the proposed model supports both approaches (different Simulink subsystems/instances are called). In both cases, the generation of a reference mission trajectory with strict timing is mandatory.

As shown in Figure 3a, the mission profile is decomposed in intervals which represent in a simplified way the signaling blocks/sections [27] in which the line is divided, for each signaling section is defined a speed limit. Blocks are defined and delimited by a vector of location nodes x_{bound}. A subset of these locations are the protected ones. The final speed of the train at each protected location is imposed. For this work, it is equal to zero.

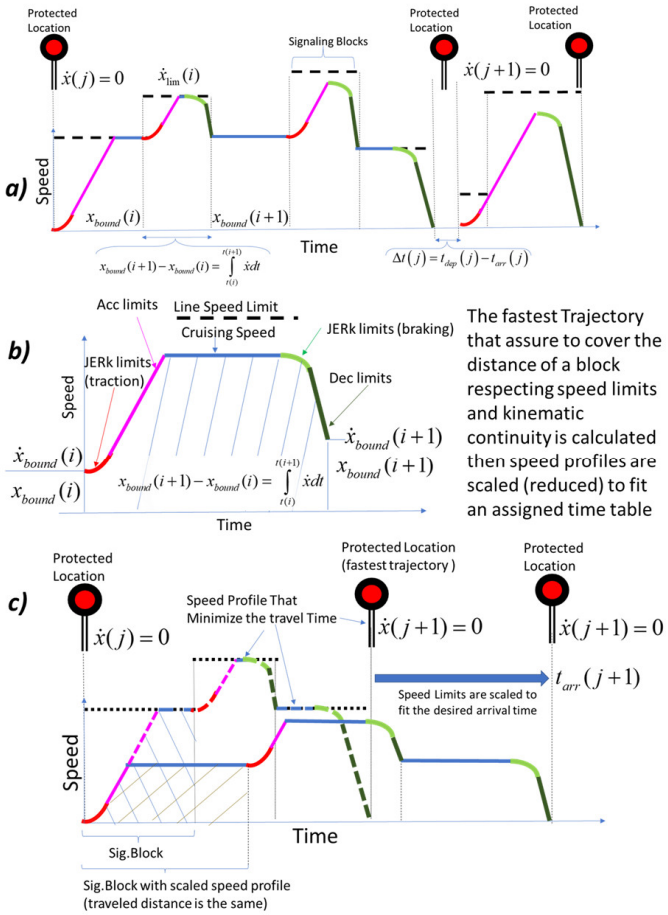

Figure 3. The mission profile with respect to blocks/sections (**a**), the mission profile of each block is treated as the summary of five different maneuvers (**b**), scaling of the speed limits to fit an assigned timetable (**c**).

As shown in Figure 3b, the trajectory of each section is decomposed in a sequence of five curves:

- A limited traction jerk trajectory: the train is accelerating with maximum jerk imposed according to the maximum traction slew rate of the simulated rolling stock.
- A limited acceleration trajectory: the train is accelerating with a maximum acceleration that respects the limits imposed by the maximum acceleration that can be calculated according to (2) by solving the Davis model:

$$\ddot{x} = \frac{T(\dot{x}, k_m)}{mk_i} - \frac{g}{k_i} i(x) - \frac{g}{k_i} i_c(x) - \frac{1}{k_i}(a\dot{x}^2 + b\dot{x} + c) - \frac{d(\dot{x} + \dot{x}_w)^2}{mk_i} \quad (3)$$

- A limited speed trajectory.
- A limited braking jerk trajectory: the train is braking with a maximum jerk imposed by the limited application rate of braking forces as stated by various standards such as, for example, fiche UIC 540 [28].
- Braking Deceleration Curve: This is the maximum deceleration that can be applied according to applied brake power and motion resistances that are also calculated according to (2).

The trajectory of each block/section is then iteratively optimized with a nested procedure: an internal loop iteratively optimizes the speed profile of each section/block, minimizing the traveling time with respect to imposed kinematic constraints (jerk, speed, and acceleration limits) and continuity on boundaries. Then, an external loop further fits the traveling time between protected locations by reshaping the speed limit constraints of signaling blocks between two protected locations. Different reshaping criteria can be applied [29] (corresponding to different optimizations). Currently, a scaling of speed limits is applied. As shown in Figure 3c, the scaled speed profile maintains the traveled distance (the integral of speed with respect to time is the same), but the new arrival time fits the desired timetable.

The total power P_{TE} can be calculated as the sum of the contribution due to traction P_{TET} (4) and electrical braking P_{TEB} (5), which respectively take count of efficiencies η_{TE} (electrical eff. of converters and motors) η_m (efficiency of mechanical transmission) and to adopted brake blending policy (k_{blend} coefficient):

$$P_{TET} = \frac{T(T > 0)\dot{x}}{\eta_{TE}\eta_m} \quad (4)$$

$$P_{TEB} = \eta_{TE}\eta_m T(T \leq 0)\dot{x}k_{blend} \quad (5)$$

The k_{blend} coefficient is calculated as the ratio between the maximum electrical braking effort T_{eb} and the total braking effort T_b, whose behavior is typically described in terms of mass-scaled efforts to equivalent deceleration, as shown in Figure 4.

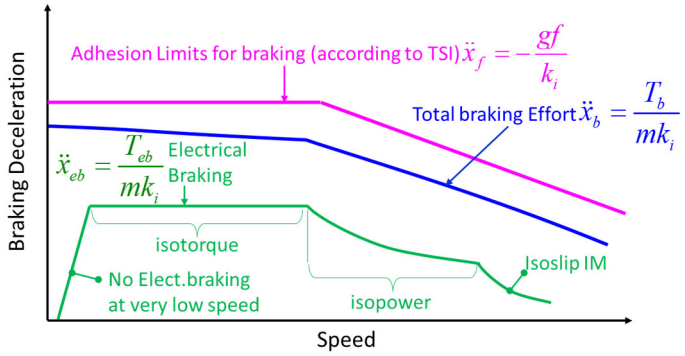

Figure 4. Braking efforts expressed in equivalent accelerations or mass scaled braking efforts.

Max equivalent deceleration permitted for allowed adhesion limits according to TSI regulations [30] is defined according to (6):

$$\ddot{x}_f = -\frac{gf}{k_i} \tag{6}$$

TSI limits described in (6) represent the maximum allowed braking performance in terms of employed wheel–rail adhesion, so total braking efforts applied to the train must be a bit lower; the associated equivalent deceleration is described by (7)

$$\ddot{x}_b = \frac{T_b}{mk_i} \tag{7}$$

With respect to the total braking performance described by (7) the maximum electrical contribution is limited by the performances of motors and converters, the resulting equivalent deceleration is described by (8).

$$\ddot{x}_{eb} = \frac{T_{eb}(\omega)}{mk_i} \tag{8}$$

In addition, in Figure 4, the typical profile of $T_{eb}(\omega)$ and consequently of equivalent acceleration is shown, evidence of some typical features:

- No electric Braking Region: for low speed (typically lower than 30 km/h), electric braking cannot be performed, so it is gradually removed with a bump-less transition.
- Constant torque Region: in this region maximum braking effort is almost constant.
- Iso Power region: when the nominal speed of the system is reached, the torque decreases with speed, describing an Iso Power Hyperbola.
- Iso-Slip region: if the motor is an induction machine, over a known speed, motor slip cannot be further increased, so the effort decreases more rapidly with a progression that is approximate to the inverse squared value of speed.

2.2. Brake Resistors Block

When electrical Braking is applied ($P_{TE} < 0$), the power generated by traction equipment can be regenerated to the primary source (as an example, sent back to the catenary through a pantograph); otherwise, it can be employed to recharge the on-board storage system or to feed auxiliary systems.

Brake Resistors are activated to dissipate the part of electric braking that cannot be allocated or regenerated to other loads. So calculation of power dissipated by brake resistors can be calculated according to (9):

$$\begin{aligned} &if(P_{TE} + P_{ESS} + P_{AUX} + P_{PPS}) \leq 0; \\ &\Rightarrow P_{BR} = -(P_{TE} + P_{ESS} + P_{AUX} + P_{PPS}) \end{aligned} \tag{9}$$

2.3. Auxiliaries

The term auxiliaries describes the loads associated with different services such as HVAC (Heating, Ventilation, and Air Conditioning), Pneumatic Braking and other pneumatic services. The statistical distribution of auxiliary loads is shown in Table 2.

Auxiliaries are an important source of consumption since, according to the literature, these loads represent at least 20% of total energy consumption for both urban [31] and conventional rail [32] transportation. Typically, auxiliary loads are treated as a mean constant load P_{AUX} (as an example, a mean consumption of 30 kW for each coach), which is applied even when the train is not moving. In addition, in this work, P_{AUX} is considered a constant load during a mission. For this reason, it is very important to take count of the

duration of stops in stations and of all the time in which for example, the rolling stock is prepared for a mission.

Table 2. Mean Statistical Distribution of Auxiliary Loads in Passenger Rolling Stock.

	Min	Mean	Max
HVAC	40%	50%	60%
Brake/Pneumatics	20%	30%	40%
Lights/Illumination	5%	10%	15%
Other Electric/Electronic Systems	5%	10%	15%

2.4. Primary Power Source

In series hybrid systems, PPS (Primary Power Sources) are devoted to supplying electric energy to other onboard subsystems by either consuming the fuel stored onboard or taking energy from external sources. For the modeling of a BEMU, the primary power source is represented by the Pantograph–Catenary current collection that feeds the vehicle under electrified lines, assuring the recharge of onboard batteries. Irreversibility and line impedance play a key role in limiting regenerative braking when the onboard storage is fully recharged since the regenerated power must be limited if line overvoltage occurs. To protect both line and rolling stock against overvoltage (corresponding to a max voltage V_{max}), the regenerated power P_{PSS} is proportionally scaled if the voltage at the pantograph V_c exceeds a threshold value Vth. The scaling factor k_{reg} is defined according to (10).

$$k_{reg} = (V_c < V_{th}) + \frac{V_c - V_{th}}{V_{\max} - V_{th}}(V_{th} \leq V_c < V_{\max}) \tag{10}$$

With regard to the traction and recharge performances, further limitations arise from the limited performance of conventional railway pantographs in collecting high currents in standstill conditions as described by current standards [33]. With regard to the modeling of the rolling stock it implies a severe limitation of static recharge performance vs the dynamic one. A limitation that can be eventually compensated by adopting the collection with multiple pantographs or with modified dedicated devices.

2.5. Storage Block

For the purpose of this work, batteries are modeled as an equivalent system whose voltage V_{bat} is described by (11) as a function of the open circuit voltage of the cells V_{oc} and of the drop because of an internal cell resistance R_{cell}. Both V_{oc} and R_{cell} are scaled according to the number of series (n_s) and parallel (n_p) connected cells that are used for the battery assembly. Battery State of Charge (SOC) is calculated according to its definition as the integral of battery currents with respect to battery capacity. With regard to the sign of current I, a positive sign corresponds to battery recharge.

$$V_{bat} = n_s V_{OC}(SOC) + R_{cell}\frac{n_s}{n_p} I_{bat} \tag{11}$$

With regard to the detailed modeling of both calendar and cycle aging, for standard simulations, this calculation is omitted. For this work, a specific approach for battery aging is fully described in the following Section 3, related to performed simulations.

If the storage block is connected to the DC bus through a static converter, efficiency is modeled, introducing a conversion efficiency $\eta_{DCDCbatt}$.

2.6. Energy Management Logic

Power management is a subsystem that is not specifically described by regulations in force [24], but it plays a mandatory role since it describes the way in which power is managed between the five subsystems described in the scheme of Figure 2.

For this work, energy management logic is described by a relatively simple set of equations according to the performed maneuver and the state of internal components and subsystems such as batteries or the availability of the primary source (the electrified line).

The input of the logic is represented by the power demand of the train P_{TR} which is defined by the sum of the power demand of both traction equipment and auxiliaries.

$$P_{TR} = P_{TE} + P_{AUX} \tag{12}$$

According to the sign of P_{TR} is possible to define the quadrant of operation of the system: if P_{TR} is positive, the train is absorbing power from the primary source and storage; otherwise is generating energy that must be dissipated or regenerated.

In the first case (P_{TR} is positive), two further subcases are possible:

- The line is electrified: P_{TR} is directly collected from the overhead line respecting the power balance (13). Where the recharge power of the battery P_{ESS} is calculated according to relation (14) and eventually saturated/limited with respect to current limits imposed by both battery BMS and by overhead line (including interposed power converters). Control (14) introduces a proportional recharge with respect to the difference between the desired maximum SOC (SOC_{lim}) and the current one.

$$P_{PPS} + P_{TR} + P_{ESS} = 0 \tag{13}$$

$$P_{ESS} = -k_{rch}(SOC_{lim} - SOC) \tag{14}$$

- The line is not electrified: all the power is provided by batteries (15). So, if P_{ESS} is not enough or the battery is depleted, system performance must be degraded.

$$P_{TR} + P_{ESS} \tag{15}$$

Otherwise, if the train has the possibility of regenerating power ($PTR < 0$), this power can be transferred to batteries, to the overhead line (if available) and then to the braking chopper (16).

$$P_{TR} + P_{PPS} + P_{ESS} + P_{BR} = 0 \tag{16}$$

Load transfer to these three alternative sinks is performed considering the following priority levels:

1. P_{ESS}: the battery is the first choice; the battery is recharged according to the maximum allowed power limits until the maximum SOC_{lim} is reached.
2. P_{PPS}: all the power exceeding the maximum performance of the battery should be regenerated to the overhead line if the train is traveling along an electrified line. If the overhead line is not able to manage the regenerated power, P_{PPS} is automatically limited according to (10).
3. P_{BR}: all the generated energy that cannot be regenerated to batteries or the overhead line is dissipated by the braking chopper. In addition, the braking chopper should have limited performance. If even the performances of the braking chopper are exceeded, electric braking will be reduced in favor of conventional pneumatic braking.

3. Battery Sizing and Simulation

3.1. Battery Sizing: Verifications of Available Weights and Encumbrances

To properly size the battery system, a preliminary evaluation of volumes and weight available on existing hybrid DMU and HMU must be performed. The main features that are considered for the benchmark train are shown in Table 3.

Table 3. Main Features of the benchmark BEMU train considered for this study.

Properties	Value
Train Mass (wheelset load)	195,000 kg
Wheelset	B_0 2 2 2 B_0
Traction Power	1557 kW
Max Traction Effort	160 kN
Nominal Speed and Effort	160 km/h, 180 kN
Max Speed	140 km/h

Available load capability and volumes that can be exploited to convert the benchmark train into a BEMU are calculated considering the removal of some components, such as the ICE power pack or the power buffer batteries.

In order to avoid the usage of potentially reserved or sensitive data, such as original CAD files, authors extrapolate available volumes from the material that was freely available online [20–22].

Most of the available volume is located on the roof of trailer coaches and in the section normally occupied by the motors.

With regard to the load capability in terms of installed batteries, it was considered a limit of no more than nine tons. This limit is quite cautious since authors must take count of the relevant weight increase that should be needed to install battery HVAC and power converters (about 20–30% of increased masses). In addition, it should be considered that these volumes and weight capabilities are distributed along the train in different locations, so sub-optimal exploitation (another 10% at least) should be expected. Starting from these roughly estimated constraints authors were able to preliminary design some Li-NMC battery packs that should respect the imposed weight and volume limits. With regard to the specifications of installed battery modules, some data shown in Table 4 have been taken from the recent technical literature [34–36] regarding batteries that are declared or claimed to be certified/assessed for railway applications.

Table 4. Investigated/Proposed battery packs that can be potentially installed on the benchmark test train.

Batt. N.	Properties
(1) [34] *Leclanche*	*Chemistry*: NMC; *Size* [kWh]: 1026.7; *Total weight*: 9006 kg; *Specific energy* [kWh/dm^3]: 113.05; *Max Charge e Discharge Rate (in C)*: 3C Discharge, 1C Charge. *Specified cycles*: 6400 (1C/1C @23 °C at 80% DoD), 3600 (1C/1C @23 °C at 100% DoD)
(2) [35] *Intilion High Pow.*	*Chemistry*: NMC; *Size* [kWh]: 1060 kWh; *Total weight*: 9048 kg *Specific energy* [kWh/dm^3]: 158.54; Max Charge e Discharge Rate (in C): 3C Discharge, 3C Charge.
(3) [36] *Lion*	*Chemistry*: NMC; *Size* [kWh]: 1352 kWh; *Total weight*: 8832 kg; *Specific energy* [kWh/dm^3]: 151.4; *Max Charge e Discharge Rate (in C)*: 3C Discharge, 3C Charge.Cycle Life: >2500 with (@25 °C ambient, 1C/1C & 100% DoD); >3000 with (@25 °C ambient, 1C/1C & 80% DoD);
(4) [37] *MG HE*	*Chemistry*: NMC; Size [kWh]: 1433.9 kWh; Total weight: 9011.8 kg; Specific energy [kWh/dm^3]: 165.4; *Max Charge e Discharge Rate (in C)*: 1C Discharge, 1C Charge. *Cycle Life*: 3000 (75% DOD), 2000 (95% DOD)
(5) [35] *IntilionHigh Energy*	*Chemistry*: NMC; *Size* [kWh]: 1600 kWh; *Total weight*: 9013.2 kg; *Specific energy* [kWh/dm^3]: 239.2; *Max Charge e Discharge Rate* (in C): 2C Discharge, 1C Charge.

3.2. Simulation of the Mission Profile: Analysis of Combined Calendar and Cycle Aging

To test the train, the line from Reggio Calabria to Catanzaro Lido is considered.

Data concerning this line are available from previous scientific publications [9].

These data have been further verified and validated by accessing open databases such as OpenRailwayMap [2], from which a large amount of information concerning electrification standards, signaling, and speed limits is available. The line is currently electrified (3 kV DC) only from Reggio Calabria to Melito P.S. (the first 30 km); the rest of the line is not electrified. Some examples of results concerning performed mission profiles are shown in Figure 5: simulated speed is much lower with respect to line speed limits since the profile is generated by real timetables that also consider some margin to recover traffic irregularities.

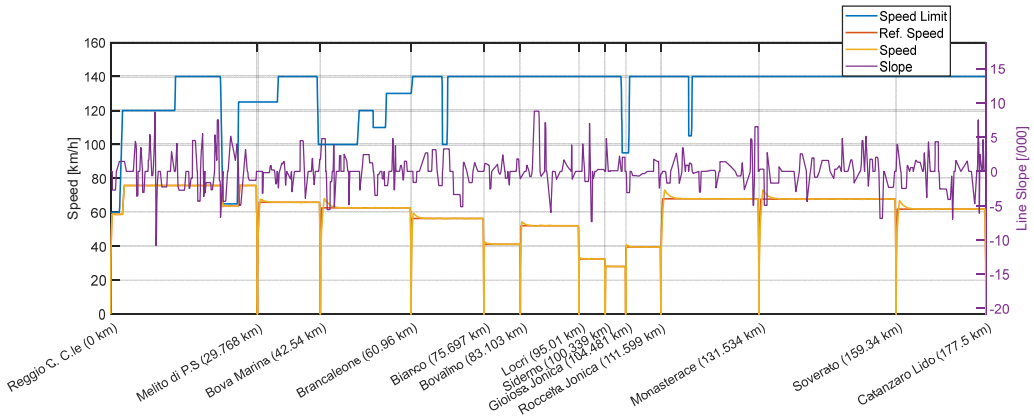

Figure 5. Simulated Mission in terms of train speed profile, slope and imposed speed limits.

Using the train model described in previous sections, it was possible to calculate a power profile associated with the mission of Figure 5. Applying the simulated load profile to batteries multiple times it is possible to calculate cycle aging. The aging calculation is performed according to the tabulated model of DE HOOG [19], which is based on wide experimental testing activities, and it is often used and cited in the literature. The model substantially introduces a tabulated current weighting for the calculation of equivalent life that is a function of several factors, including current and temperature, as the most important ones.

With regard to aging, isothermal behavior is assumed (it is supposed to be an ideal thermal conditioning plant for batteries). Thanks to the relatively fast execution of the proposed model, authors can analyze the cumulated effects of cycle and calendar aging over the whole life of the battery.

This study investigates both calendar and cycle aging, so it was necessary to associate a typical mission profile both with traveled mileage and elapsed time.

This association is performed considering the combined mission profile of Table 5. This profile is relatively cautious with regard to aging since the battery is continuously used without considering the idle time that should be inevitably associated with maintenance activities and suboptimal scheduling (a typical employment time of about 10% should be considered). However, this very cautious margin should compensate for uncalculated calendar aging associated with suboptimal usage of the rolling stock: when rolling stock is idle, calendar aging is still working, also considering that without mitigative actions such as the control of a low conservative SOC of accumulators or some care to protect storages from extreme temperatures, calendar aging should be even accelerated.

Table 5. Simulated Mission Profile.

Property	Feature
Reggio C. Catanzaro L.	Trip/day: 2
Catanzaro L. Reggio C.	Trip/day: 2
Recharge	Only at the end of the line
Duration of Stops at the end of the line	30 min for the largest battery, 40–65 min for the smallest.
Total km/day	Total km: 710 km Total km under electrified: 119 km Total km under not electrified line: 591 km Tot Time: 15 h for largest batt., 17 h for smallest one
Total Service Time	Time elapsed with the train stopped in the railway station: 3 h for largest batt, 4 h 30 min for smallest one.
Day of service/week	7
Added Time for Maintenance Interval	None

The results concerning the combined calendar and cycle aging of different battery packs are shown in Figure 6: Expected service duration in the day for different battery packs is compared considering the separated and combined actions of cycle and calendar aging. The battery life is considered "ended" when capacity falls under 80% of its original value. To extend the life of batteries, it is supposed to be a normal use in which a reduced SOC range from 20 to 80%. This assumption reduces the maximum autonomy by about 40% but contributes to increasing the life of the cells in a significant way. However, it also assures a practical safety margin for real working conditions, where an extended duration of the mission due to traffic perturbations is possible. For this work, if SOC falls under the minimum level of 20%, this safety margin is exploited to end the mission, but the pack is considered unreliable for the proposed service profile.

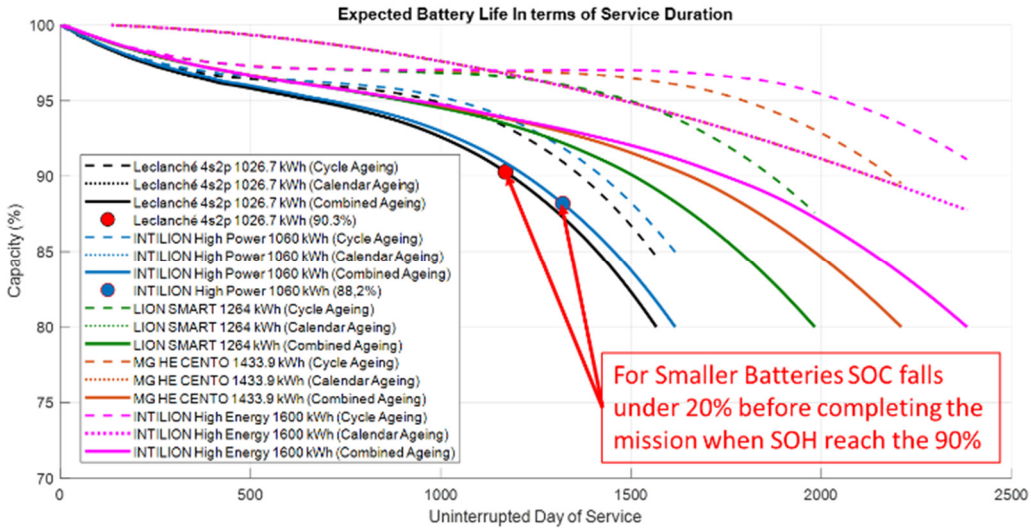

Figure 6. Simulated combined cycle and calendar aging of different LiNMC Batteries (dotted lines corresponding to pure calendar aging are equal since the same aging model is applied).

Looking at the experimental results of Figure 6, it can be observed that the largest battery packs are subjected to slower cycle aging, so their foreseen life is longer (7 years of cont. service). For smaller battery packs, capacity fading may lead to operational conditions in which the SOC of the battery falls under the minimum limit of 20% when battery SOH (ratio between current and Nominal Capacity) is still 90%; the battery has not reached EOL (End Of Life) but to complete the mission, a minimum safety SOC of 20% must be

overridden. Rolling stock is functional (at the end of the mission there is a residual positive SOC), but autonomy is not enough to complete the mission respecting imposed SOC limits.

As the foreseen life of the storage life increases, the difference between combined aging (calendar and cycle) and cycle aging also increases. It can be concluded that for large battery packs with LiNMC technology calendar aging must be carefully minimized. So, it is fundamental to improve thermal conditioning and battery balancing to protect the storage from calendar ageing. This consideration also poses a limit to the maximum size of the storage system, since a "too big" battery should be over-penalized by calendar aging.

3.3. Introduction of a Dynamic Recharge Island

Starting from the results of Figure 6, the authors argued that to reduce equivalent costs related to calendar aging of LiNMC batteries, a reduction in the pack should be implemented. At the same time, a reduction in the battery pack should be over-penalized in terms of cycle aging because the train is unable to complete the mission when the battery is still relatively new (90% of the original capacity is about half of the expected life). So, the authors evaluate the possibility of introducing an intermediate electrified section of a few kilometers (7 km for the purpose of the simulation) in which the rolling stock is dynamically recharged. The choice of a dynamic recharge island is supported by the following fundamental considerations:

- With respect to a static recharge station, no time is wasted.
- During the recharge, the train is moving, so a part of the energy is directly used for traction, further improving battery life, efficiency, and autonomy.
- Infrastructural costs are higher; however, there is no need to add dedicated recharge devices that are less standardized with respect to fully interoperable components used for conventional "pure" electric trains. So, the impact in terms of additional weight and complexity of the system is reduced.
- Dynamic Recharge is much more convenient if conventional railway pantograph and overhead lines are used since the maximum currents that can be collected are about ten times greater.
- Finally, the current autonomy of trains with standard LTO batteries

The chosen positioning of the recharge station is optimized by minimizing the maximum DOD (Degree of discharge of the battery). For the chosen mission profile in which the altimetric gradients of the line are very small (the line is almost plain), the optimal position is substantially not influenced by the motion sense and corresponds (for a single intermediate recharge island) to placement at about a half of the non-electrified section of the line, as shown in Figure 7. This is not a trivial consideration since for mountain lines for which slopes and reached altitudes are not negligible [4], the optimal positioning of the intermediate electrified sections should be much more complicated and sensitive to motion sense along the line.

With regard to the length of the intermediate section, in this work, the authors have considered the minimal one (7 km) that should allow a complete recharge of the battery pack (results of Figure 7 are referred to as battery pack 5 of Table 4). Probably, further optimization should be performed considering the trade-off between the costs of involved infrastructure and gains in terms of improved reliability of involved rolling stock.

The simulation campaign was then repeated, considering the introduction of the intermediate recharge section along the line. Some results are shown in Figure 8: simulation has been carried out for the two smaller battery packs, which are the most penalized by cycle aging.

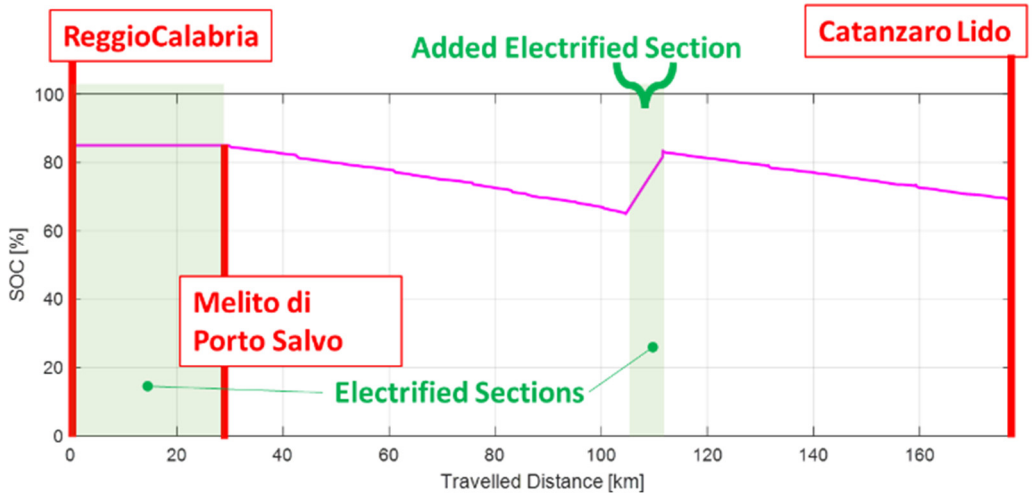

Figure 7. Supposed Intermediate Recharge Section (simulated SOC behavior for the largest installed battery).

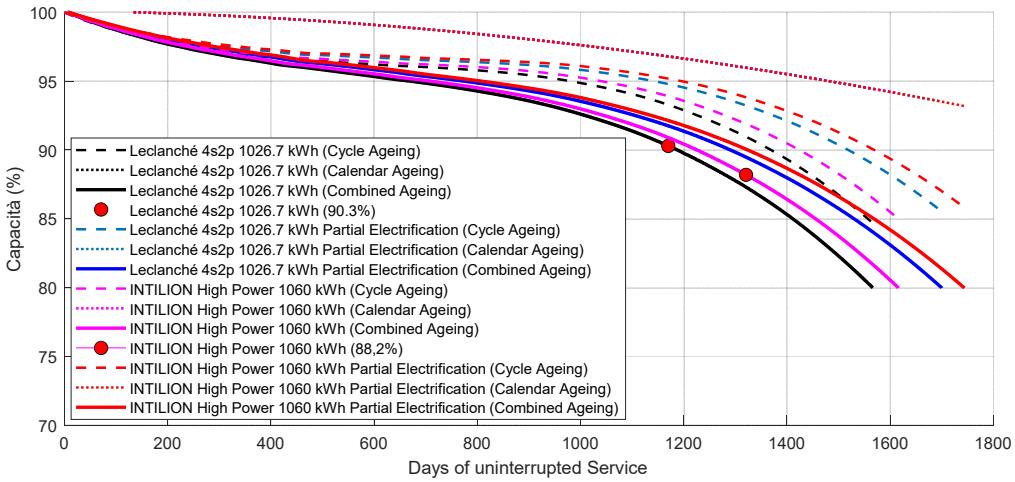

Figure 8. Life Extension of smaller battery packs with an intermediate electrified section of 7 km to perform the dynamic recharge of the battery (dotted lines corresponding to pure calendar aging are equal since the same aging model is applied).

Added electrified section (7 km) corresponds to a reduction of about 5% of traveled distance under not electrified lines. In addition, the energy flow that affected cycle aging is reduced by about 5%. However, the calculated extension of life with the introduced partial electrification is greater than expected:

- For battery pack 1, the life extension considering combined calendar and cycle aging is 9%.
- For battery pack 2, the life extension is at least 8%.
- For both battery packs neglecting calendar aging, the improvements in terms of cycle aging are about 10–11%

So, despite calendar aging, the improvement in terms of cycle aging is quite better than expected. Reducing the maximum DOD of batteries, a significant improvement in terms of expected life is verified.

For both storages, even when the battery is relatively near to EOL, the minimum SOC limit of 20% is always respected, so the mission profile is completed, maintaining a safe energy margin. The proposed solution (intermediate electrification of the line) is also compatible with the adoption of conventional BEMUs equipped with LTO cells for

which autonomy of about 70–100 km is commonly expected. So, it can be concluded that the insertion of relatively short, electrified sections along the line should be an interesting choice that should allow an extended and more reliable service for both Li-NMC and LTO-powered solutions.

4. Conclusions

In this work, the authors have successfully investigated the application of aging models to the design of storage for a railway application. Current results are interesting and provide the system designer with potentially useful data that can be used to design the process of BEMU. According to the proposed results, the usage of LiNMC cells allows the construction of BEMUs with higher autonomy that can tolerate a continuous service life from 5 to 8 years, according to traffic intensity and performed mission. LiNMC batteries are relatively more sensitive to calendar aging with respect to LTO ones, so calendar aging is also much more important: a further increase in the storage size should probably penalize this aspect with respect to involved costs and investment. With respect to the foreseen life of BEMUs (for rolling stock of at least 20–30 years), this solution involves the necessity of a periodical substitution of batteries. However, it should be considered that the cost of LiNMC is about one-fifth/one-tenth of a corresponding solution with LTO (so there is an economic margin for battery substitution). In addition, it should be considered the development trend of battery technology and, consequently, the availability in a few years of even more performing cells or sustainable cells [38].

So, authors believe that the calculated life of the LiNMC pack is acceptable, also considering the continuous evolution of battery cells that should make near to mandatory an update of cell and BMS technology at least every ten to fifteen years. In this sense, the main issue is represented by the necessity of periodic updates of the homologation of safety-relevant components such as batteries. This process, in the opinion of authors, can be accelerated by admitting the extended application of simulation instruments/digital twins of the proposed battery pack integrated with HIL testing performed on Roller Rigs [39] (also with regard to the mechanical performances) or in large scale device currently used to verify auxiliary behavior and overall system reliability in harsh weather/environmental conditions [40].

Author Contributions: Conceptualization, L.P.; Methodology, L.P. and N.T.; Software, T.E.P. and N.T.; Validation, N.T.; Writing—original draft, L.P.; Visualization, L.P. and T.E.P.; Supervision, L.P.; Project administration, L.P.; Funding acquisition, L.P. All authors have read and agreed to the published version of the manuscript.

Funding: This study was carried out within the MOST—Sustainable Mobility National Research Center and received funding from the European Union Next-Generation EU (PIANO NAZIONALE DI RIPRESA E RESILIENZA (PNRR)—MISSIONE 4 COMPONENTE 2, INVESTIMENTO 1.4—D.D. 1033 17/06/2022, CN00000023). This manuscript reflects only the authors' views and opinions; neither the European Union nor the European Commission can be considered responsible for them.

Data Availability Statement: The raw data supporting the conclusions of this article will be made available by the authors on request.

Conflicts of Interest: The authors declare no conflicts of interest.

Abbreviations

P_{TE}	Power requested or regenerated by Traction Equipment
P_{BR}	Power dissipated by the braking Chopper
P_{AUX}	PPower consumed by on board auxiliaries
P_{PPS}	PPower exchanged with the Primary Power Source

P_{ESS}	Power exchanged with the on board storage system
T	Longitudinal effort applied to the Train Composition
$x, \dot{x}, \ddot{x}, \dddot{x}$	Longitudinal displacement and its derivatives (speed, acceleration and jerk)
m	Train mass
g	Gravitational acceleration
i, i_c	Line slope and equivalent slopes introduced by lumped resistances such as curves and switches
a, b, c, d	Coefficients of distributed motion resistances
$\dot{x}_w$	Longitudinal Component of Wind Speed
k_m	Long. Effort conf. Parameter
k_i	Ratio between equivalent translational inertia and train mass
$\ddot{x}_f$	Equivalent max deceleration associated to the max adhesion limits prescribed by TSI (Technical Specification for Interoperability)
$\ddot{x}_b$	Equivalent max deceleration associated to total braking performances
$\ddot{x}_{eb}$	Equivalent max deceleration related only to electrical braking
$V_c, V_{th}, V_{\max}$	Voltage level of collected current at the pantograph and corresponding threshold and maximum values
V_{bat}, I_{bat}	Voltage and Current of the Battery pack
$V_{OC}(SOC)$	Open circuit voltage of a cell, modeled as a function of SOC (State Of Charge)
n_s, n_p	Number of cells connected in series and parallel in the battery pack
$\eta_{DCDCbat}$	Efficiency of battery static converter stage
$SOC_{\lim}$	Maximum recharge reference limit for battery recharge controller
k_{rch}	Prop. Gain of the battery recharge controller

References

1. Zenith, F.; Isaac, R.; Hoffrichter, A.; Thomassen, M.S.; Møller-Holst, S. Techno-economic analysis of freight railway electrification by overhead line, hydrogen and batteries: Case studies in Norway and USA. *Proc. Inst. Mech. Eng. Part F J. Rail Rapid Transit* **2020**, *234*, 791–802. [CrossRef]
2. OpenRailwayMap Official Site. Available online: https://www.openrailwaymap.org/ (accessed on 20 October 2024).
3. Du, Y. Large models in transportation infrastructure: A perspective. *Intell. Transp. Infrastruct.* **2024**, *3*, liae007. [CrossRef]
4. Pugi, L.; di Carlo, L. Multi-modal battery-operated trains on partially electrified lines: A case study on some regional lines in Italy. *Proc. Inst. Mech. Eng. Part F J. Rail Rapid Transit* **2024**, *238*, 09544097241234959. [CrossRef]
5. Herrera, V.I.; Gaztañaga, H.; Milo, A.; Saez-de-Ibarra, A.; Etxeberria-Otadui, I.; Nieva, T. Optimal energy management and sizing of a battery—Supercapacitor-based light rail vehicle with a multiobjective approach. *IEEE Trans. Ind. Appl.* **2016**, *52*, 3367–3377. [CrossRef]
6. Barbosa, F.C. Fuel cell rail technology review: A tool for an autonomous rail electrifying strategy. In Proceedings of the ASME/IEEE Joint Rail Conference, Snowbird, UT, USA, 9–12 April 2019; American Society of Mechanical Engineers: New York, NY, USA, 2019; Volume 58523, p. V001T07A001.
7. Cole, C.; Sun, Y.; Wu, Q.; Spiryagin, M. Exploring hydrogen fuel cell and battery freight locomotive options using train dynamics simulation. *Proc. Inst. Mech. Eng. Part F J. Rail Rapid Transit* **2024**, *238*, 310–321. [CrossRef]
8. Ahsan, N.; Hewage, K.; Razi, F.; Hussain, S.A.; Sadiq, R. A critical review of sustainable rail technologies based on environmental, economic, social, and technical perspectives to achieve net zero emissions. *Renew. Sustain. Energy Rev.* **2023**, *185*, 113621. [CrossRef]
9. Fragiacomo, P.; Piraino, F.; Genovese, M.; Flaccomio Nardi Dei, L.; Donati, D.; Migliarese Caputi, M.V.; Borello, D. Sizing and performance analysis of hydrogen-and battery-based powertrains, integrated into a passenger train for a regional track, located in Calabria (Italy). *Energies* **2022**, *15*, 6004. [CrossRef]
10. Pugi, L.; Berzi, L.; Spedicato, M.; Cirillo, F. Hydrogen for railways: Design and simulation of an industrial benchmark study. *Int. J. Model. Identif. Control.* **2023**, *43*, 43–53. [CrossRef]
11. Deng, K.; Liu, Y.; Hai, D.; Peng, H.; Löwenstein, L.; Pischinger, S.; Hameyer, K. Deep reinforcement learning based energy management strategy of fuel cell hybrid railway vehicles considering fuel cell aging. *Energy Convers. Manag.* **2022**, *251*, 115030. [CrossRef]
12. Bauer, R.; Reimann, S.; Gratzfeld, P. Modeling of Traction Batteries for Rail Applications Using Artificial Neural Networks. In Proceedings of the 2021 IEEE Transportation Electrification Conference & Expo (ITEC), Chicago, IL, USA, 21–25 June 2021; IEEE: Piscataway, NJ, USA, 2021; pp. 826–831.

13. Davoodi, M.; Jafari Kaleybar, H.; Brenna, M.; Zaninelli, D. Energy Management Systems for Smart Electric Railway Networks: A Methodological Review. *Sustainability* **2023**, *15*, 12204. [CrossRef]
14. Vignati, M.; Debattisti, N.; Bacci, M.L.; Tarsitano, D. A software-in-the-loop simulation of vehicle control unit algorithms for a driverless railway vehicle. *Appl. Sci.* **2021**, *11*, 6730. [CrossRef]
15. Ruvio, A.; Martirano, L.; Galasso, A.; Vescio, G. Comparing Battery and Hybrid Diesel-Battery Freight Trains for Heavy Industrial. In Proceedings of the 2024 IEEE International Conference on Environment and Electrical Engineering and 2024 IEEE Industrial and Commercial Power Systems Europe (EEEIC/I&CPS Europe), Rome, Italy, 17–20 June 2024. [CrossRef]
16. Nemeth, T.; Schröer, P.; Kuipers, M.; Sauer, D.U. Lithium titanate oxide battery cells for high-power automotive applications–electro-thermal properties, aging behavior and cost considerations. *J. Energy Storage* **2020**, *31*, 101656. [CrossRef]
17. Brady, M. *Assessment of Battery Technology for Rail Propulsion Application*; Technical Report No. DOT/FRA/ORD-17/12; Federal Railroad Administration: Washington, DC, USA, 2017.
18. Cuma, M.U.; Yirik, E.; Dericioğlu, Ç.; Ünal, E.; Onur, B.; Tumay, M. Design considerations of high voltage battery packs for electric buses. *Int. J. Adv. Automot. Technol.* **2017**, *1*, 73–79. [CrossRef]
19. de Hoog, J.; Timmermans, J.M.; Ioan-Stroe, D.; Swierczynski, M.; Jaguemont, J.; Goutam, S.; Omar, N.; Van Mierlo, J.; Van Den Bossche, P. Combined cycling and calendar capacity fade modeling of a Nickel-Manganese-Cobalt Oxide Cell with real-life profile validation. *Appl. Energy* **2017**, *200*, 47–61. [CrossRef]
20. Vannucchi, A. HITACHI RAIL STS SPA. La Piattaforma MASACCIO di Hitachi Rail per la Decarbonizzazione dei Treni Regionali. Webinar at Expo Ferroviaria Free Presentation. Available online: www.cifi.it/UplDocumenti/Milano29092021/04Vannucchi.pdf (accessed on 20 December 2024).
21. Sacchi, M. Responsabile HITACHI RAIL ITALY—Piattaforma Rolling Stock il Nuovo Treno Ibrido per Trenitalia Caratteristiche Tecniche—Il Punto di Vista HITACHI RAIL ITALY. Official CIFI Webinar Held on 21/04/2022. Available online: https://www.cifi.it/UplDocumenti/Firenze21042022/Il%20nuovo%20treno%20ibrido%20per%20Trenitalia.pdf (accessed on 20 December 2024).
22. Caposciutti, M. Responsabile Trenitalia—Direzione Tecnica Il Nuovo Treno Ibrido per TreniatalisL Nuovo Treno Ibrido Caratteristiche Tecniche—Il Punto di Vista Trenitalia. Webinar Held on 21/04/2022. Available online: https://www.cifi.it/UplDocumenti/Firenze21042022/Presentazione%20Trenitalia.pdf (accessed on 20 December 2024).
23. Pugi, L.; Berzi, L.; Cirillo, F.; Vecchi, A.; Pagliazzi, V. A tool for rapid simulation and sizing of hybrid traction systems with fuel cells. *Proc. Inst. Mech. Eng. Part F J. Rail Rapid Transit* **2023**, *237*, 104–113. [CrossRef]
24. *IEC 62864-1:2016*; Railway Applications—Rolling Stock—Power Supply with Onboard Energy Storage System—Part 1: Series Hybrid System. ISO: Geneva, Switzerland, 2016.
25. Cole, C.; Spiryagin, M.; Wu, Q.; Sun, Y.Q. Modelling, simulation, and applications of longitudinal train dynamics. *Veh. Syst. Dyn.* **2017**, *55*, 1498–1571. [CrossRef]
26. Wang, J.; Rakha, H.A. Longitudinal train dynamics model for a rail transit simulation system. *Transp. Res. Part C Emerg. Technol.* **2018**, *86*, 111–123. [CrossRef]
27. Theeg, G.; Vlasenko, S. *Railway Signalling & Interlocking*; International Compendium; PMC Media House GmbH: Leverkusen, Germany, 2009; p. 448.
28. Fiche UIC 540. *Brakes Air Brakes for Freight Trains and Passenger Trains*, 7th ed.; UIC: Paris, France, 2016.
29. Fernández, P.M.; Sanchís, I.V.; Yepes, V.; Franco, R.I. A review of modelling and optimisation methods applied to railways energy consumption. *J. Clean. Prod.* **2019**, *222*, 153–162. [CrossRef]
30. Commission Regulation (EU). No 1302/2014 of 18 November 2014 concerning a technical specification for interoperability relating to the rolling stock—Locomotives and passenger rolling stock subsystem of the rail system in the European Union. *Off. J. Eur. Union* **2014**, *L 356*, 228.
31. González-Gil, A.; Palacin, R.; Batty, P.; Powell, J.P. A systems approach to reduce urban rail energy consumption. *Energy Convers. Manag.* **2014**, *80*, 509–524. [CrossRef]
32. Douglas, H.; Roberts, C.; Hillmansen, S.; Schmid, F. An assessment of available measures to reduce traction energy use in railway networks. *Energy Convers. Manag.* **2015**, *106*, 1149–1165. [CrossRef]
33. *IRS 60608 Conditions to be Complied with for the Pantographs of Tractive Units Used in International Services*, 1st ed.; UIC: Paris, France, 2019.
34. LECLANCHE-plaquette-G-NMC-KMWEB.pdf. Available online: https://www.leclanche.com/wp-content/uploads/2020/10/LECLANCHE-plaquette-G-NMC-KMWEB.pdf (accessed on 20 December 2024).
35. Intilion Datasheet. Rail_hv-modul_data_sheet_de.pdf. Available online: https://www.hoppecke.com/fileadmin/Redakteur/Hoppecke-Main/Products-Import/rail_hv-modul_data_sheet_de.pdf (accessed on 20 December 2024).
36. Lion Smart Datasheet. 202409_Datasheet_LION-Smart-Mobility-Power-42-1. Available online: https://lionsmart.com/wp-content/uploads/2024/06/202406_Datasheet-LION-Smart-Mobility-Power-42.pdf (accessed on 20 December 2024).
37. MG HE 100 Datasheet. Available online: https://www.mgenergysystems.eu/en/products/he-series/ (accessed on 20 December 2024).

38. Titirici, M.; Johansson, P.; Ribadeneyra, M.C.; Au, H.; Innocenti, A.; Passerini, S.; Petavratzi, E.; Lusty, P.; Tidblad, A.A.; Naylor, A.J.; et al. 2024 roadmap for sustainable batteries. *J. Phys. Energy* **2024**, *6*, 041502. [CrossRef]
39. Malvezzi, M.; Allotta, B.; Pugi, L. Feasibility of degraded adhesion tests in a locomotive roller rig. *Proc. Inst. Mech. Eng. Part F J. Rail Rapid Transit* **2008**, *222*, 27–43. [CrossRef]
40. Bucek, O. Research on the comprehensive climate environment test methods for railway vehicles in climate wind tunnel. In Proceedings of the 2017 2nd International Conference on Industrial Aerodynamics (ICIA 2017), Qingdao, China, 18–20 October 2017; pp. 11–20.